Phase separation and metal-insulator transitions in the spin-$\frac{1}{2}$ Falicov-Kimball model

Pavol Farkašovský
Institute of Experimental Physics, Slovak Academy of Sciences, Watsonova 47, 043 53 Košice, Slovakia
(Received 20 January 1999; revised manuscript received 1 June 1999)

The ground-state phase diagram of the spin-$\frac{1}{2}$ Falicov-Kimball model (FKM) is studied in one dimension using small-cluster exact-diagonalization calculations. The resultant exact solutions are used to examine possibilities for valence and metal-insulator transitions in this model. A number of remarkable results are found. (i) The phase separation in the spin-$\frac{1}{2}$ FKM takes place for a wide range of *f*-electron concentrations n_f and *d*-*f* interactions G, including G large. (ii) In the strong-coupling limit ($G>4$) the model exhibits a pressure-induced discontinuous insulator-metal transition from an integer-valence state ($n_f=1$) into another integer-valence state ($n_f=0$). (iii) For intermediate values of G ($G\sim 2.5$) the FKM undergoes a few discontinuous intermediate-valence transitions. There are several discontinuous insulator-insulator transitions from $n_f=1$ to $n_f=1/2$ and a discontinuous insulator-metal transition from $n_f=1/2$ to $n_f=0$. (iv) In the weak-coupling limit ($G<2$) the model undergoes a few consecutive discontinuous and continuous intermediate-valence transitions as well as a discontinuous metal-insulator transition. [S0163-1829(99)12339-7]

I. INTRODUCTION

Recent measurements of the insulator-metal transitions in SmB_6 (Ref. 1) and in the transition-metal halides[2] have once again sparked an interest in valence and insulator-metal transitions.[3] These transitions are observed in a wide group of substances formed by transition-metal oxides as well as rare-earth sulfides and borides, when some external parameters (like pressure or temperature) are varied. They are in many cases first-order phase transitions; however, second-order transitions ranging from very gradual to rather steep are also observed.[4]

To describe all such transitions in a unified picture Falicov and Kimball[5] introduced a simple model in which only two relevant single-electron states are taken into account: extended Bloch waves and a set of localized states centered at the sites of the metallic ions in the crystal. It is assumed that insulator-metal transitions result from a change in the occupation numbers of these electronic states, which remain themselves basically unchanged in their character. The Hamiltonian of the model can be written as the sum of four terms,

$$H_0=\sum_{ij\sigma} t_{ij} d^{\dagger}_{i\sigma} d_{j\sigma}+G\sum_{i\sigma\sigma'} f^{\dagger}_{i\sigma} f_{i\sigma} d^{\dagger}_{i\sigma'} d_{i\sigma'}+E_f\sum_{i\sigma} f^{\dagger}_{i\sigma} f_{i\sigma} + \frac{U}{2}\sum_{i\sigma} f^{\dagger}_{i\sigma} f_{i\sigma} f^{\dagger}_{i-\sigma} f_{i-\sigma}, \quad (1)$$

where $f^{\dagger}_{i\sigma}$, $f_{i\sigma}$ are the creation and annihilation operators for an electron of spin σ in the localized state at lattice site i with binding energy E_f and $d^{\dagger}_{i\sigma}$, $d_{i\sigma}$ are the creation and annihilation operators of the itinerant electrons in the *d*-band Wannier state at site i.

The first term of Eq. (1) is the kinetic energy corresponding to quantum-mechanical hopping of the itinerant *d* electrons between sites i and j. These intersite hopping transitions are described by the matrix elements t_{ij}, which are $-t$ if i and j are the nearest neighbors and zero otherwise (in the following all parameters are measured in units of t). The second term represents the on-site Coulomb interaction between the *d*-band electrons with density $n_d=N_d/L=(1/L)\Sigma_{i\sigma} d^{\dagger}_{i\sigma} d_{i\sigma}$ and the localized *f* electrons with density $n_f=N_f/L=(1/L)\Sigma_{i\sigma} f^{\dagger}_{i\sigma} f_{i\sigma}$, where L is the number of lattice sites. The third term stands for the localized *f* electrons whose sharp energy level is E_f. The last term represents the intra-atomic Coulomb interaction between the localized *f* electrons.

It should be noted that in addition to the FKM there are other two-band models (e.g., the Anderson model and the Kondo model) used in the literature for a description of valence and metal-insulator transitions. Unlike the FKM that emphasizes the role of the interband Coulomb interaction (and ignores all effects arising from the hybridization between the localized and the conduction-band orbitals) the Anderson and the Kondo model emphasize the role of the interband hybridization. At present, it remains unclear whether it is the electronic system, modeled by the FKM, that is driving the transition, or whether it is driven by other (hybridization or electron-phonon) effects. Recently, the question about discontinuous transitions in the spin-$\frac{1}{2}$ FKM has been answered in the affirmative for the special case of infinite dimensions by Chung and Freericks.[6] Here we examine the opposite limit ($d=1$) and only the zero-temperature properties of the model are discussed.

In spite of the fact that the FKM is one of the simplest examples of interacting fermionic system, the theoretical picture of valence and insulator-metal transitions remains still uncertain in the framework of this model. Even in the existing literature on this model, different answers can be found on the fundamental question whether the FKM can describe both the discontinuous and continuous changes of the *f*- (d)-electron occupation number n_f (n_d) as a function of the *f*-level energy E_f.[7] It should be noted that this question is indeed crucial for the systems mentioned above, since, supposing[4] that the external pressure shifts the energy level E_f, the valence changes observed in some rare-earth and transition-metal compounds (SmS, SmB_6, Ti_2O_3, and so on) could be understandable purely electronic. Unfortunately, it was found that valence and insulator-metal transitions are

very sensitive to the approximation used. Various approximations[7] [mean-field, virtual crystal, coherent-potential (CPA), etc.] yield very different and often fully controversial results. This indicates that the study of valence and insulator-metal transitions may be successful only with methods that are relatively insensitive to the type of approximation used and, of course, with exact methods.

In our previous papers[8,9] we have showed that the method of small-cluster exact-diagonalization calculations is very effective in describing ground-state properties of both the spinless and spin-$\frac{1}{2}$ FKM. For the spinless FKM (Ref. 8) the exact numerical calculations (over the full set of *f*-electron configurations) can be performed on relatively large clusters ($L\sim 36$), even without some special computational effort. For such clusters the finite-size effects are practically negligible and the results can be satisfactory extrapolated to the thermodynamics limit ($L\rightarrow\infty$). Using this method we have described successfully the ground-state phase diagram as well as the picture of valence and metal-insulator transitions in the spinless FKM.[8] The situation for the spin-$\frac{1}{2}$ FKM is more complicated. The full Hilbert space of the spin-$\frac{1}{2}$ FKM is much larger than one of the spinless FKM and this fact imposes severe restrictions on the size of clusters that can be studied by the exact-diagonalization method. Our recent[9] numerical computations performed for the spin-$\frac{1}{2}$ FKM with U and G finite showed that clusters with $L>24$ are beyond the reach of present day computers. Fortunately, the size of the Hilbert space can be reduced considerably in some special, but physically still interesting, limits, e.g., $U\rightarrow\infty$. In the limit $U\rightarrow\infty$ states with two *f* electrons at the same site are projected out, thereby much larger clusters ($L\sim 36$) become accessible for the numerical investigation in this reduced subspace. For this reason all calculations presented in this paper have been done at $U=\infty$. The main goal for performing these calculations was to construct the comprehensive phase diagram of the spin-$\frac{1}{2}$ FKM. The second goal of our numerical study was to find and describe all possible types of valence and metal-insulator transitions in this model. We show that both the ground-state phase diagram as well as the picture of valence and metal-insulator transitions obtained for $U=\infty$ strongly differ from ones obtained in our previous paper[9] for a restricted set of *f*-electron configurations and U finite. In particular, the exhaustive numerical studies of the model (at $U=\infty$) performed on finite clusters up to 36 sites revealed some unexpected features like the phase separation for all nonzero G and discontinuous metal-insulator transitions for G small, to mention only a few. In the present paper we discuss these features in detail.

Since the *f*-electron density operators $f^{\dagger}_{i\sigma}f_{i\sigma}$ of each site i commute with the Hamiltonian (1), the *f*-electron occupation number is a good quantum number, taking only two values, $w_i=0,1$ according to whether the site i is unoccupied or occupied by the localized *f* electron (configurations with $w_i=2$ are projected out due to $U=\infty$). Therefore the Hamiltonian (1) can be replaced by

$$H=\sum_{ij\sigma} h_{ij}d^{\dagger}_{i\sigma}d_{j\sigma}+E_f\sum_i w_i, \qquad (2)$$

where $h_{i,j}=t_{ij}+Gw_i\delta_{ij}$.

Thus for a given *f*-electron configuration $w=\{w_1,w_2\ldots w_L\}$ defined on a one-dimensional lattice with periodic boundary conditions, the Hamiltonian (2) is the second-quantized version of the single-particle Hamiltonian $h(w)=T+GW$, so the investigation of the model (2) is reduced to the investigation of the spectrum of h for different configurations of *f* electrons. Since the *d* electrons do not interact among themselves, the numerical calculations precede directly in the following steps (we consider only the case $N_f+N_d=L$, which is the point of the special interest for valence and metal-insulator transitions caused by promotion of electrons from localized *f* orbitals ($f^n\rightarrow f^{n-1}$) to the conduction-band states). (i) Having G, E_f, and $w=\{w_1,w_2\ldots w_L\}$ fixed, we find all eigenvalues λ_k of $h(w)=T+GW$. (ii) For a given $N_f=\Sigma_i w_i$ we determine the ground-state energy $E(w)=\Sigma_{k=1}^{L-N_f}\lambda_k+E_fN_f$ of a particular *f*-electron configuration w by filling in the lowest $N_d=L-N_f$ one-electron levels (the spin degeneracy must be taken into account). (iii) We find the w^0 for which $E(w)$ has a minimum. Repeating this procedure for different values of N_f, G, and E_f, one can immediately study the ground-state phase diagram of the model in the N_f-G plane as well as the dependence of the *f*-electron occupation number $N_f=\Sigma_i w_i^0$ on the *f*-level position E_f (valence transitions).

II. PHASE SEPARATION

In this section we study the ground-state phase diagram of the spin-$\frac{1}{2}$ FKM in the n_f-G plane for $E_f=0$. This phase diagram is the spin analogy of the canonical phase diagram found by Gruber *et al.*[10] for the spinless FKM and it plays the important role in theoretical studies of the model, for both $E_f=0$ and $E\neq 0$. Indeed, the spectrum of $h(w)=T+GW$ does not depend on E_f and thus all nonzero E_f properties of the model can be directly calculated from the zero E_f phase diagram. For example, knowing the n_f-G phase diagram (i.e., the ground-state configurations for each N_f and G) for $E_f=0$, one can easily compute the E_f dependence of n_f (at fixed G), since only L configurations (instead of the full set of 2^L configurations) must be examined numerically at each E_f point, thereby the numerical calculations are considerably simplified.

To reveal the basic structure of the phase diagram in the N_f-G plane ($E_f=0$) we have performed an exhaustive study of the model on finite (even) clusters up to 36 sites. For fixed L the numerical calculations have been done along the lines discussed above with a step $\Delta N_f=2$ and $\Delta G=0.05$. The results of numerical computations are summarized in Fig. 1. These results show that the phase diagram of the spin-$\frac{1}{2}$ FKM consists of three main domains: the most homogeneous domain (MHD) (in Fig. 1 denoted as $\cdot$) and two-phase separation domains PSD_1 (denoted as $\bigcirc$, $\times$, and $+$) and PSD_2 (denoted as $\triangle$). In the MHD the ground states are configurations in which the atomic or *n*-molecule clusters of *f* electrons are distributed in such a manner that the distances between two consecutive clusters are either d or $d+2$. Furthermore, the distribution of the distances of d and $d+2$ has to be most homogeneous. Two basic types of the ground-state configurations that fill up practically the whole MHD are displayed in Table I. In the PSD_1 the ground

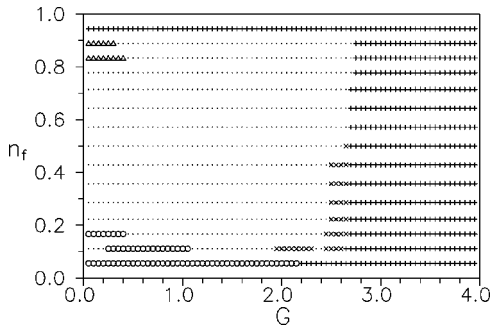

FIG. 1. Ground-state phase diagram of the spin-$\frac{1}{2}$ FKM obtained over the full set of *f*-electron configurations. For $1/4<n_f<3/4$ numerical calculations have been done on the lattice with $L=28$ while for $n_f \leqslant 1/4$ and $n_f \geqslant 3/4$ they have been done on the lattice with $L=36$. Four different regions of stability corresponding to mixtures $w_a \& w_e$, $w_b \& w_e$, $w_c \& w_e$, and $w_d \& w_f$ are denoted as $\bigcirc$, $\times$, $+$, and $\triangle$.

states are configurations in which all *f* electrons are distributed only in one part of the lattice (w) while another (connecting) part of the lattice (w_e) is free of *f* electrons (phase separation). In accordance with Gruber *et al.*[10] we call such configurations mixtures and denote them as $w \& w_e$. Of course, for finite systems this abbreviation has only formal meaning, since all ground-state quantities (e.g., the ground-state energy) are calculated directly from the spectrum of $h(w \& w_e)$ and not from the weighted densities of states corresponding to w and w_e as for thermodynamic systems. We have found three basic types of configurations w which form these mixtures: (i) the aperiodic atomic configurations $w_a=\{10_{k_1}10_{k_2}\ldots 10_{k_i}1\ldots 0_{k_2}10_{k_1}1\}$ (with $k_i>0$), (ii) the aperiodic n_i-molecule configurations $w_b=\{1_{n_1}0_{k_1}1_{n_2}0_{k_2}\ldots 1_{n_i}0_{k_i}1_{n_i}\ldots 0_{k_2}1_{n_2}0_{k_1}1_{n_1}\}$ (with $1 \leqslant n_i \leqslant N_f/2$ and $k_i>0$), and (iii) the N_f-molecule (segregated) configurations $w_c=\{11\ldots 1\}$. Three different regions of stability corresponding to mixtures $w_a \& w_e$, $w_b \& w_e$, and $w_c \& w_e$ are denoted in Fig. 1 as $\bigcirc$, $\times$, and $+$. It is seen that the mixtures of the atomic configuration w_a and the empty configuration are stable only at low *f*-electron concentrations and the Coulomb interactions $G<2.2$. A direct comparison of results obtained for the spin-$\frac{1}{2}$ and spinless FKM (Ref. 10) shows that this region corresponds roughly to a region of phase separation in the spinless FKM. Outside these regions the phase diagrams of the spin-$\frac{1}{2}$ and spinless FKM are,

TABLE I. Two basic types of the most homogeneous configurations that fill up practically the whole MHD for $L=24$.

N_f	w_h^a	w_h^b
4	100001000000100001000000	110000000000110000000000
6	100100001001000010010000	110000001100000011000000
8	100100100100100100100100	110000110000110000110000
10	110010011001001001100100	110011000011001100110000
12	110011001100110011001100	110011001100110011001100
14	111001110011100111001100	
16	111100111100111100111100	
18	111111001111110011111100	
20	111111111100111111111100	

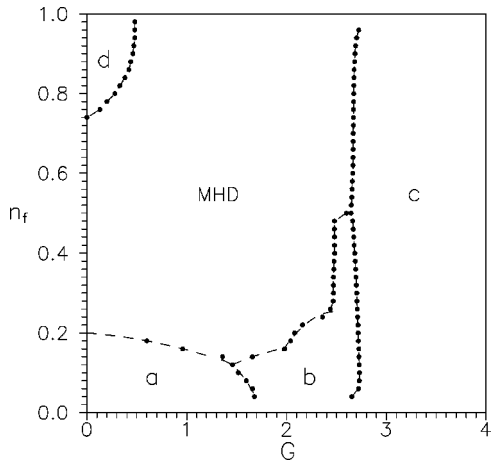

FIG. 2. Ground-state phase diagram of the spin-$\frac{1}{2}$ FKM obtained on the extrapolated set of *f*-electron configurations for $L=100$. Four different regions of stability corresponding to mixtures $w_a \& w_e$, $w_b \& w_e$, $w_c \& w_e$, and $w_d \& w_f$ are denoted as *a*, *b*, *c*, and *d*. The dashed line through the exact numerical points is a guide to the eye.

however, strongly different. While the phase separation in the spinless FKM takes place only for weak interactions ($G<1.2$), the spin-$\frac{1}{2}$ FKM exhibits the phase separation for all Coulomb interactions. Even with increasing G the phase separation shifts to higher *f*-electron concentrations. Particularly, in the region $2.5<G<2.7$ where the ground states are the mixtures of the *n*-molecule configurations w_b with the empty configuration the phase separation takes place for all $N_f<L/2$, and in the region $G>2.7$ where the ground states are the segregated configurations $w_S=w_c \& w_e$ even for all $N_f<L$. At large *f*-electron concentrations n_f but in the opposite limit ($G<0.4$) there exists another small domain of the phase separation PSD_2 (denoted as $\triangle$). The numerical results on finite lattices up to 36 sites revealed only one type of configuration that can be the ground-state configurations in this domain, and namely, the mixtures of the periodic *n*-molecule configurations w_d with the fully occupied lattice $w_f=\{11\ldots 1\}$ (the length of a connected cluster of occupied sites in these mixtures is at least $L/2$).

The second step in our numerical studies has been the extrapolation of small-cluster exact diagonalization results on large lattices. In Fig. 2 we present the ground-state phase diagram of the spin-$\frac{1}{2}$ FKM obtained for $L=100$ on the extrapolated set of configurations that includes practically all possible types of the ground-state configurations found on finite lattices up to 36 sites. In particular, we have considered (i) the most homogeneous configurations w_h of the type *a* and *b* (see Table I), (ii) all mixtures $w_a \& w_e$ with k_i smaller than 6, (iii) all mixtures $w_b \& w_e$ with n_i and k_i smaller than 6, (iv) all mixtures $w_d \& w_f$ with periods smaller than 12, and (v) all segregated configurations. One can see that all fundamental features of the phase diagram found on small lattices hold on much larger lattices, too. Of course, the phase boundaries of different regions corresponding to mixtures $w_a \& w_e$ (*a*), $w_b \& w_e$ (*b*), $w_c \& w_e$ (*c*), and $w_d \& w_f$ (*d*) are now more obvious. Since the mixtures $w_a \& w_e$, $w_b \& w_e$, $w_c \& w_e$, and $w_d \& w_f$ are metallic[10] one can expect that the phase boundary between the MHD and PSD is also the boundary of the correlation-induced metal-insulator transi-

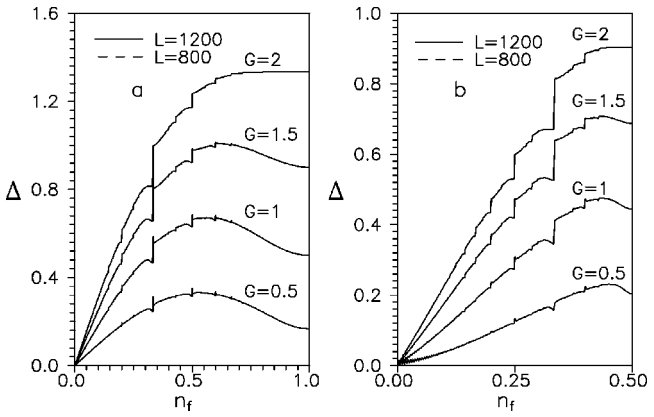

FIG. 3. n_f dependence of the energy gap Δ calculated for the most homogeneous configurations of the type *a* and *b* (see Table I).

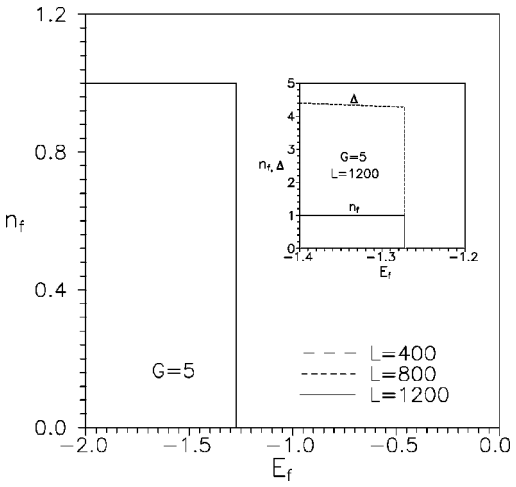

FIG. 4. Dependence of the *f*-electron occupation number n_f on the *f*-level position E_f for $G=5$ and three different values of L. Inset: The behavior of n_f and Δ close to the insulator-metal transition point.

tion. To confirm this conjecture it is necessary to show that the most homogeneous configurations from the MHD are insulating or, in other words, that there is a finite energy gap Δ at the Fermi energy in the spectra of these configurations.[11] The numerical results for the most homogeneous configurations of types *a* and *b* that fill up practically the whole MHD are displayed in Fig. 3. The insulating character of these configurations is clearly demonstrated by the finite Δ that exists for all nonzero *f*-electron concentrations n_f and Coulomb interactions G. Thus we can conclude that the spin-$\frac{1}{2}$ FKM undergoes (on the phase boundary between the MHD and PSD) the correlation-induced metal-insulator transition that is accompanied by a discontinuous change of the energy gap Δ. This result is similar to what was found for the spinless FKM by numerical[10] and analytical calculations in the strong-[12] and weak-coupling limit.[13]

III. VALENCE AND METAL-INSULATOR TRANSITIONS

The existence of a large metallic domain in the strong-coupling region is the main difference between the phase diagram of the spin-$\frac{1}{2}$ and spinless FKM. In the spinless FKM (Ref. 10) the existence of the metallic phase was restricted only on a small region $G<1.2$ and $n_f<1/4$ ($n_f>3/4$), while the remaining part of the phase diagram was insulating. The phase diagram of the spin-$\frac{1}{2}$ FKM has a more complicated structure. In addition to the insulating phase corresponding to the homogeneous configurations w_h there are four metallic phases corresponding to four different classes of the ground-state configurations: $w_a \& w_e$, $w_b \& w_e$, $w_c \& w_e$, and $w_d \& w_f$. Of course, this fact has to also lead to a different picture of valence and metal-insulator transitions induced by pressure (increasing E_f). Let us now discuss, in more detail, possible types of these transitions. In order to examine possible types of valence and insulator-metal transitions induced by pressure we have chosen three different values of G ($G=1, 2.5, 5$) that represent three typical regimes of the spin-$\frac{1}{2}$ phase diagram. For $G=5$ the valence transition can be constructed immediately. Indeed the ground states in this region are only the segregated configurations and thus they can be used directly in numerical calculations instead of the full set of *f*-electron configurations. This allows us to perform numerical calculations on large systems and practically fully exclude finite-size effects. Results of numerical calculations are shown in Fig. 4. It is seen that in the strong-coupling limit the spin-$\frac{1}{2}$ FKM exhibits a discontinuous valence transition from an integer-valence ground state $n_f=1$ into another integer-valence ground state $n_f=0$ at $E_f=E_c\sim 1.273$. The inset in Fig. 4 shows that the discontinuous valence transition is accompanied by a discontinuous insulator-metal transition since the energy gap Δ vanishes discontinuously at $E_f=E_c$. Thus we can conclude that the spin-$\frac{1}{2}$ FKM in the pressure-induced case can describe the discontinuous insulator-metal transitions from an integer-valence state ($n_f=1$) into another integer-valence state ($n_f=0$). It should be noted that the same picture of valence and metal-insulator transitions in the strong coupling limit was found by Chung and Freericks[6] for the infinite-dimensional case. The only difference between these two pictures is that the discontinuous transitions from the noninteracting insulating phase to the noninteracting metallic phase take place at different values of E_f ($E_f=4/\pi$ in our case).

The situation for $G=2.5$ is slightly complicated. Although we know that the ground states for $2.45<G<2.75$ (and $n_f<1/2$) are configurations of a type $w_b \& w_e$, the number of configurations belonging to this class is still too large for numerical calculations on large lattices and thus it should be further reduced. For this reason we have performed numerical calculations for all finite (even) clusters up to 48 sites at selected value $G=2.5$. We have found that for any $N_f>0$ only one type of configuration and namely mixtures $\{11001100\ldots1100\} \& w_e$ are the ground states at $G=2.5$. This allows us to avoid technical difficulties associated with a large number of configurations and consequently to study very large systems ($L\sim 1200$). The valence transition obtained for this set of configurations (and w_h configurations for $n_f>1/2$) is shown in Fig. 5. It is seen that the valence transition for $G=2.5$ is very steep. A more detail analysis showed, however, that the transition from $n_f=1$ to $n_f=0$ is not a discontinuous integer-valence transition but it consists of several discontinuous intermediate-valence transitions. Particularly, there are several discontinuous insulator-insulator transitions from $n_f=1$ to $n_f=1/2$ and a discontinuous insulator-metal transition from $n_f=1/2$ to $n_f=0$. To ex-

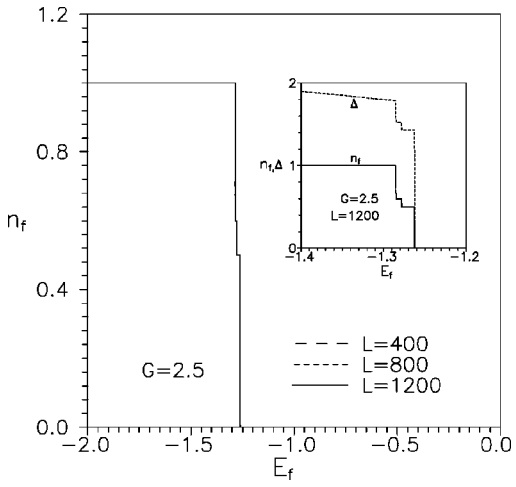

FIG. 5. Dependence of the *f*-electron occupation number n_f on the *f*-level position E_f for $G=2.5$ and three different values of L. Inset: The behavior of n_f and Δ close to the insulator-metal transition point.

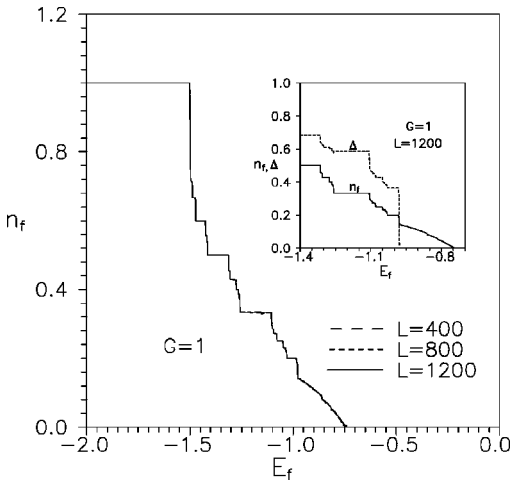

FIG. 6. Dependence of the *f*-electron occupation number n_f on the *f*-level position E_f for $G=1$ and three different values of L. Inset: The behavior of n_f and Δ close to the insulator-metal transition point.

clude the possibility that this structure is a consequence of the finite size of clusters used in numerical calculations we have performed calculations on several large clusters ($L=400,800,1200$) but no significant finite-size effects on the valence transition were observed.

The most complicated situation is for small and intermediate values of G. For example, at the selected value of $G=1$ the ground states are the insulating configurations w_h (for $n_f>0.16$) and the metallic configurations $w_a \& w_e$ (for $n_f<0.16$). However, for a construction of the valence transition on large lattices this knowledge is too general and thus for $n_f<n_c$ it is again necessary to perform an additional study of the model in order to determine the explicit type of ground-state configurations at selected value of G. The exhaustive numerical studies that we have performed for $n_f<n_c$ on finite lattices up to 60 sites showed that only configurations of the type $w_1=\{1010_{n_1}1010_{n_2}\ldots 0_{n_2}1010_{n_1}101\}\&w_e$ or configurations of the type $w_2=\{10_{n_1}1010_{n_2}1010_{n_3}\ldots 0_{n_3}1010_{n_2}1010_{n_1}1\}\&w_e$ can be the ground states at $G=1$. This fact allows us to use the set of configurations w_1 and w_2 instead of the much larger set $w_a \& w_e$ and consequently to construct the valence transition on large lattices ($L\sim 1200$). The results of numerical calculations obtained for the E_f dependence of the *f*-electron occupation number n_f and the energy gap Δ are displayed in Fig. 6. Unlike the valence transitions obtained for $G=5$ and $G=2.5$ the valence transitions in the weak-coupling limit are much wider and consist of several consecutive discontinuous and continuous valence transitions. The valence transitions for $E_f<E_c\sim -1.05$ are insulator-insulator transitions since they realize between insulating ground states corresponding to the most homogeneous configurations w_h. At $E_f=E_c$ the spin-$\frac{1}{2}$ FKM undergoes a pressure-induced discontinuous valence transition from an intermediate valence state with $n_f\sim 0.19$ into another intermediate-valence state with $n_f\sim 0.14$ that is accompanied by a discontinuous insulator-metal transition. Above E_c the *f*-electron occupation number n_f changes continuously and vanishes at $E_f=E_0\sim -0.8$.

It should be noted that the weak-coupling picture of valence and metal-insulator transitions presented in this paper strongly differs from the one found in our previous work[9] for the restricted set of configurations consisting of only the most homogeneous configurations w_h. For such a set of configurations the system exhibits the metal-insulator transition only at $E_f=E_0$ and this transition is continuous. This fact indicated the serious deficiency of the spin-$\frac{1}{2}$ FKM since in some rare-earth compounds [e.g., in SmB_6 (Ref. 1)] just a discontinuous insulator-metal transition is observed. Fortunately, a more accurate analysis performed in the present paper has not confirmed this deficiency of the model. On the contrary, our numerical results showed that the spin-$\frac{1}{2}$ FKM is capable of describing not only a discontinuous metal-insulator transition but all basic types of valence transitions observed experimentally in rare-earth and transitions-metal compounds. This indicates that the spin-$\frac{1}{2}$ FKM could yield the correct physics for describing these materials. However, to make definite conclusions one should examine the model in higher dimensions, since most experimental systems are two and three dimensional. Moreover, in this paper we discussed only the zero-temperature properties of the model and it still remains an open question whether this model is capable of describing the nonzero-temperature behavior of rare-earth and transition-metal compounds. Recent results of Chung and Freericks[6] obtained in the limit of infinite dimensions show that the answer to this question could be positive at least for some anomalous behaviors that exhibit these compounds, e.g., the temperature dependence of the *d*-electron occupation number (conductivity).

In summary, the extrapolation of small-cluster exact-diagonalization calculations has been used to examine the ground-state phase diagram of the spin-$\frac{1}{2}$ FKM in the one dimension. A number of remarkable results have been found. (i) The phase separation in the spin-$\frac{1}{2}$ FKM takes place for a wide range of *f*-electron concentrations n_f and *d*-*f* interactions G, including G large. (ii) In the strong-coupling limit ($G>4$) the model exhibits a pressure-induced discontinuous

insulator-metal transition from an integer-valence state ($n_f = 1$) into another integer-valence state ($n_f = 0$). (iii) For intermediate values of G ($G \sim 2.5$) the FKM undergoes a few discontinuous intermediate-valence transitions. There are several discontinuous insulator-insulator transitions from $n_f = 1$ to $n_f = 1/2$ and a discontinuous insulator-metal transition from $n_f = 1/2$ to $n_f = 0$. (iv) In the weak-coupling limit ($G < 2$) the model undergoes a few consecutive discontinuous and continuous intermediate-valence transitions as well as a discontinuous metal-insulator transition.

This work was supported by the Slovak Grant Agency VEGA under Grant No. 2/4177/97.

[1] J.C. Cooley, M.C. Aronson, Z. Fisk, and P.C. Canfield, Phys. Rev. Lett. **74**, 1629 (1995).

[2] M.P. Pasternak, R.D. Taylor, A. Chen, C. Meade, L.M. Falicov, A. Giesekus, R. Jeanloz, and P.Y. Yu, Phys. Rev. Lett. **65**, 790 (1990); A.L. Chen, P.Y. Yu, and R.D. Taylor, *ibid.* **71**, 4011 (1993).

[3] J.K. Freericks and L.M. Falicov, Phys. Rev. B **45**, 1896 (1992); A. Giesekus and L.M. Falicov, *ibid.* **44**, 10 449 (1991).

[4] D.L. Khomskii, in *Quantum Theory of Solids*, edited by I.M. Lifshitz (Mir, Moscow, 1982).

[5] L.M. Falicov and J.C. Kimball, Phys. Rev. Lett. **22**, 997 (1969).

[6] W. Chung and J.K. Freericks, Phys. Rev. B **57**, 11 955 (1998).

[7] C.E.T. Goncalves da Silva and L.M. Falicov, J. Phys. C **9**, 906 (1972); J. Rossler and R.J. Ramirez, *ibid.* **9**, 3747 (1976); J.W. Schweitzer, Phys. Rev. B **17**, 758 (1977); M. Plischke, Phys. Rev. Lett. **28**, 361 (1972); D.K. Ghosh, Solid State Commun. **18**, 1377 (1976); A.C. Hewson and P.S. Reiseborough, *ibid.* **22**, 379 (1977).

[8] P. Farkašovský, Phys. Rev. B **51**, 1507 (1995); **52**, R5463 (1995).

[9] P. Farkašovský, Phys. Rev. B **54**, 11 261 (1996).

[10] Ch. Gruber, D. Ueltschi, and J. Jedrzejewski, J. Stat. Phys. **76**, 125 (1994).

[11] Since we consider the case $N_f + N_d = L$, the Fermi level E_F and the energy gap Δ of some configuration w are given by $E_F = \lambda_{L-N_f}$ and $\Delta = \lambda_{L-N_f+1} - \lambda_{L-N_f}$, respectively.

[12] P. Lemberger, J. Phys. A **41**, 715 (1992).

[13] J.K. Freericks, Ch. Gruber, and N. Macris, Phys. Rev. B **53**, 16 189 (1996).